ChemComm

Accepted Manuscript

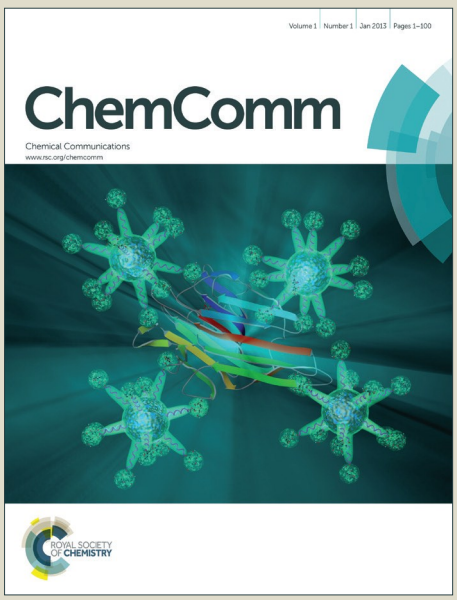

ROYAL SOCIETY OF CHEMISTRY

www.rsc.org/chemcomm

Chemical Communications

RSCPublishing

COMMUNICATION

Polymerizable Supramolecular Approach to Fabricating Patterned Magnetic Nanoparticles

Cite this: DOI: 10.1039/x0xx00000x

Joosub Lee[a], Ki-Seung Seo[a], Chan Woo Lee*[b] and Jong-Man Kim*[a,b]

Received 00th January 2015,
Accepted 00th January 2015

DOI: 10.1039/x0xx00000x

www.rsc.org/

A simple and highly effective method for fabricating patterned magnetic nanoparticles was developed. The procedure utilizes a UV irradiation-wet etching-calcination sequence starting with a magnetic nanoparticle embedded polymerizable diacetylene film.

Superparamagnetic materials are intrinsically nonmagnetic but are magnetically activated in the presence of an external magnetic field. Functional magnetic nanoparticles (MNPs) have been extensively investigated in the context of applications in the areas of sensing, imaging, separation and purification.[1-7] In addition, several approaches have been developed for fabrication of patterned magnetic nanoparticles, [8-10] including microcontact printing (μCP),[11,12] capillary filling,[13] photolithography,[14,15] block copolymer lithography[16] as well as site-selective deposition[17] and dewetting.[18] However, these methods suffer from one or more limitations associated with complicated fabrication procedures, the use of sophisticated and expensive instrumentation, poor resolution and thickness control difficulties. In the study described below, we have devised a simple and efficient approach for constructing patterned NMPs that relies on the use of polymerizable supramolecules.

Lipid molecules containing a diacetylene (DA) unit tend to self-assemble to form well-ordered supramolecular structures. Irradiation of the DA lipid supramolecules with 254 nm UV light induces a 1,4-addition polymerization process that generates polymerized DA supramolecules called polydiacetylenes (PDA).[19-22] In general, PDAs are blue colored as a consequence of absorption wavelength maximum around 650 nm caused by the presence of an extensive array of overlapping p-orbitals. Interestingly, PDAs readily undergo a blue-to-red color change upon various (bio)chemical (organic solvents, pH, ligand-receptor interaction, etc.) and physical (heat, mechanical strain) stimuli. [23-38]

During recent studies aimed at the development of PDA-based smart materials,[39-42] we explored an intriguing PDA based strategy for the fabrication of patterned magnetite nanoparticles (MNPs). As is depicted schematically in Fig. 1, photomasked UV irradiation of a thin DA film containing embedded MNPs should result in selective photopolymerization to yield PDAs in UV exposed areas. Since PDAs are insoluble in common organic solvents, incubation of the UV exposed film in organic solution is expected to remove DA in the unirradiated areas exclusively. Finally, calcination at high temperatures should remove all organic materials, leaving behind patterned MNPs.

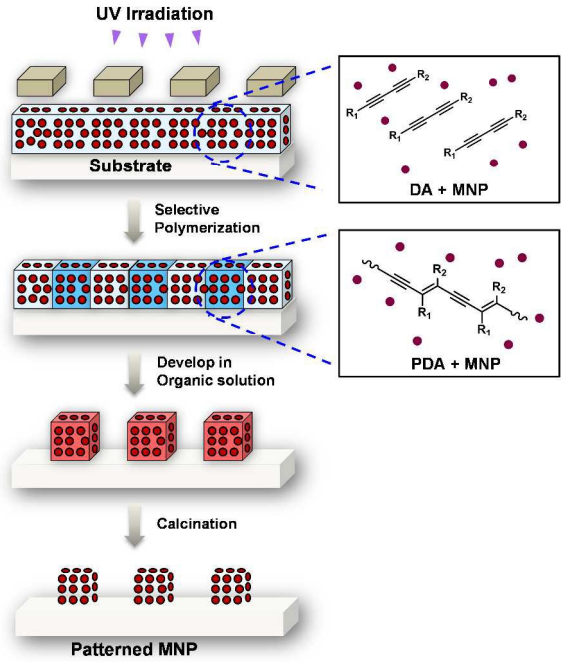

Fig. 1 Schematic representation of a new approach for the fabrication of patterned magnetic nanoparticles.

In order to investigate the feasibility of the proposed polymerizable supramolecular approach for patterned MNP fabrication, a thin DA film was prepared by spin-coating a chloroform solution containing 10,12-pentacosadiynoic acid [PCDA, $CH_3(CH_2)_{11}C{\equiv}C\text{-}C{\equiv}C(CH_2)_8COOH$] (3

wt%) and MNP (3 wt%) (Fig. 2A). The diacetylenic lipid, PCDA, was selected for this purpose because it is commercially available and it is known to form self-assembled supramolecular lamellar structures readily. In addition, PCDA-derived supramolecules can be polymerized by irradiation with 254 nm UV light. Magnetite (Fe_3O_4) nanoparticles of ca. 20 nm diameter were prepared employing a known procedure[43,44] (Fig. S1, ESI†) and then coated with PCDA (see ESI†). Addition of a THF solution containing PCDA to the in-situ generated MNPs in water results in formation of PCDA-coated MNPs after washing with MeOH and re-dispersion in heptane.

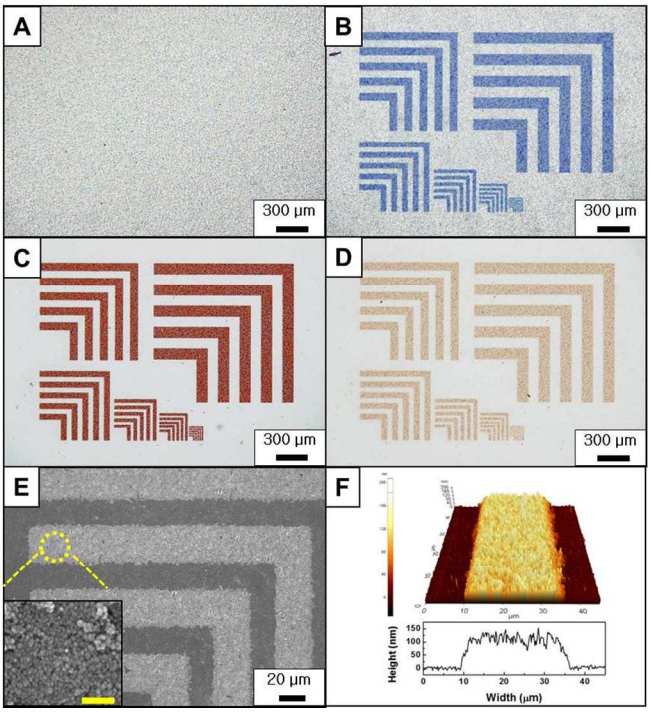

Fig. 2 (A-D) Optical microscopic images of a thin film containing PCDA (3 wt%) and magnetite nanoparticles (3 wt%) on a glass substrate as prepared (A), after 254 nm UV irradiation for 20 min (B), after development in THF (C), and after calcination at 400 °C for 2 h (D). (E) SEM image of patterned magnetite nanoparticles. The scale bar in the inset of the figure is 100 nm. (F) AFM image and cross sectional profile of a magnetite film.

Photomasked UV irradiation (254 nm, 12.5 mW/cm^2) of the magnetite-containing PCDA film for 20 min results in the generation of blue-colored patterns on the solid substrate (Fig. 2B). The appearance of the easily recognized blue color is typical for PDA generation. Incubation of the blue patterned film in organic solvents (THF followed by acetone) causes removal of unpolymerized PCDA as well as MNPs embedded in the PCDA matrix in photomasked areas, leaving behind MNP-embedded PDA in photoirradiated areas of the glass slide In addition, a blue-to-red color transition of the patterned images occurs during the wet etching step (Fig. 2C) as a consequence of dissolution of unpolymerized residual DA monomers and partially polymerized oligomers in THF. These processes create voids in the PDA supramolecules resulting in partial distortion of the polymer backbone and disruption of conjugation. Polymer side chains are altered by rotation about carbon-carbon single bonds in the main backbone and this leads to shortening of the effective conjugation length.

Calcination of the glass substrate results in generation of patterned, yellow-brown colored magnetite nanoparticles (Fig. 2D). It should be noted that a yellow-brown pattern is not produced when a PCDA film not containing embedded magnetite nanoparticles are subjected to the irradiation-etching-calcination process. This observation demonstrates that the patterned images are associated with magnetite (Fig. S2, ESI†). In addition, thermogravimetric (TG) (Fig. S3, ESI†) and energy dispersive X-ray (EDX) spectroscopic (Fig. S4, ESI†) analyses show that all carbon-containing substances are removed during the calcination step.

The patterned magnetite nanoparticles were also analysed by using scanning electron microscopy (SEM) and atomic force microscopy (AFM) (Fig. 2E and 2F). The SEM image (Fig. 2E) shows that micron sized finely patterned magnetite nanoparticles are present. The bright areas in the SEM image represent magnetite nanoparticles obtained after calcination and the inset figure shows aggregated magnetite nanoparticles. Moreover, the AFM image and height profile displayed in Fig. 2F show that the magnetite nanoparticles are present only in UV exposed areas. The resolution of magnetite patterning is dependent on the resolution of the photomask used. Because of this limitation, the smallest nanoparticle patterns we were able to generate have sizes of ca. 20 micron (Fig. S5, ESI†).

UV-Vis spectroscopic monitoring of the magnetite patterning process confirms that blue-phase PDAs, which have a maximum absorption wavelength at 640, are generated by UV irradiation (Fig. S6, ESI†). In addition, this analysis demonstrates that a spectral shift to a shorter wavelength takes place after the wet-etching step. Furthermore, the absorption band associated with the PDA completely disappears upon calcination.

One meritorious feature of newly developed strategy for MNP patterning is that the thickness of NMPs can be readily manipulated by varying the amount of NMPs. It is clear from viewing the height profiles displayed in Fig. 3 that the thickness of the magnetite nanoparticles obtained after calcination increases in a manner that is directly proportional to the amount of MNPs used. Specifically, the thickness of the magnetite nanoparticles are *ca.* 50 nm when 1 wt% of magnetite nanoparticles is employed while the use of 2 wt% leads to production of a 75 nm thickness and a maximum thickness of 105 nm is generated when 3 wt% magnetite nanoparticles is employed.

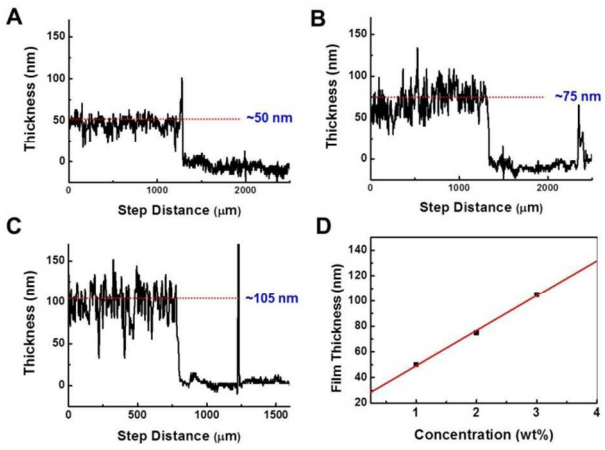

Fig. 3 (A-C) Height profiles of the magnetic nanoparticles derived from the use of 1 wt% (A), 2 wt% (B), and 3 wt% (C) magnetite. The amount of PCDA used is fixed at 3 wt%. (D) Plot of height as a function of magnetite concentration.

It should be noted that increases in the thickness of the nanoparticles results in the generation of more defects on the surfaces of the magnetite nanoparticles (Fig. S7, ESI†).

The properties of MNPs fabricated by employing the new polymerizable supramolecular approach were monitored by using X-ray diffraction (XRD) spectroscopy (Fig. 4A). The XRD spectrum of a thin film of pure PCDA contains several distinct peaks below 24° (Fig. 4A, a) and the spectrum of a thin film comprised of both PCDA and magnetite nanoparticles contains peaks corresponding to both components (Fig. 4A, b). After calcination, the peaks associated with PCDA disappear leaving behind only those arising from magnetite nanoparticles (Fig. 4A, c), a conclusion that is confirmed by comparison with the XRD spectrum of independently prepared magnetite nanoparticles (Fig. 4A, d). Analysis of the hysteresis curve (Fig. 4B) of nanoparticles obtained from the sequential UV irradiation-etching-calcination process shows that a typical magnetic response takes place, thus, confirming the effectiveness of the new strategy (see also Fig. S8, ESI† for hysteresis curves for pure magnetite nanoparticles and PCDA-coated magnetic nanoparticles). It should be noted that the superparamagnetic activity of the magnetic nanoparticles is slightly lower (ca. 10%) after calcination

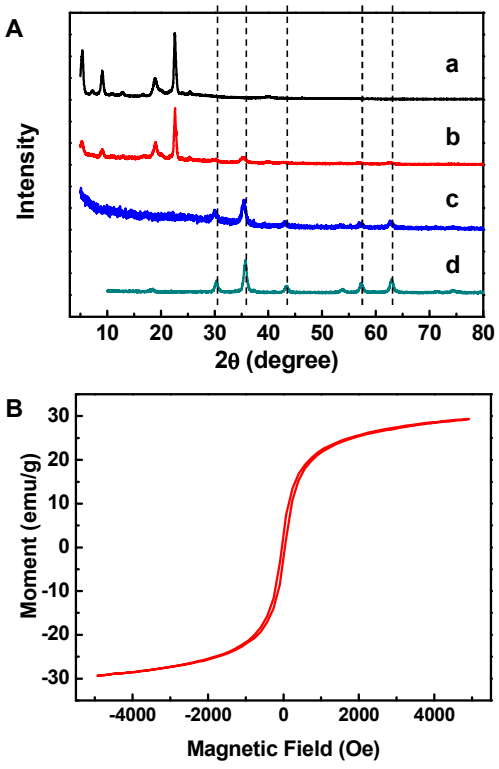

Fig. 4 (A) XRD patterns of PCDA (a), PCDA-MNP composite film (b), the PCDA-MNP composite film obtained after calcination (c), and magnetite nanoparticles (d). (B) A hysteresis curve of magnetite nanoparticles obtained from a sequential UV irradiation-etching-calcination process of a PCDA-MNP composite film.

In conclusion, in the effort described above we developed a straightforward polymerizable supramolecular method for the preparation of patterned MNPs. The new approach, which utilizes photomasked UV-irradiation of an MNP-embedded diacetylene film followed by employment of a sequential wet etching-calcination process, enables fabrication of finely patterned MNPs on a solid substrate. Moreover, because each step yields a distinct color corresponding to the PDA (blue and red) and MNP (yellow-brown), the patterning process can be readily monitored by using the naked eye. Finally, the thickness of the MNP film can be readily manipulated by controlling the amount of NMP employed. We believe that the new methodology will be applicable to the fabrication of other types of metallic nanoparticles and, as a result, it will serve as the foundation for new applications of PDA.

This work was supported by the National Research Foundation of Korea (NRF) grant funded by the Korea government (MSIP) (No. 2014R1A2A1A01005862 and 2012R1A6A1029029).

Notes and references

[a] *Department of Chemical Engineering, Hanyang University, Seoul 133-791, Korea. E-mail: jmk@hanyang.ac.kr*
[b] *Institute of Nano Science and Technology, Hanyang University, Seoul 133-791, Korea. E-mail: lcw@hanyang.ac.kr*

† Electronic Supplementary Information (ESI) available: Experimental details and supporting figures. See DOI: 10.1039/c000000x/

1. J. Guo, W. Yang, C. Wang, *Adv. Mater.*, 2013, **25,** 5196.
2. O. V. Kharissova, H. V. R. Dias, B. I. Kharisov, *RSC. Adv.*, 2015, **5**, 6695.
3. S. Das, P. Ranjan, P. S. Maiti, G. Singh, G. Leitus, R. Klajn, *Adv. Mater.*, 2013, **25**, 422.
4. J. Gallo, N. Kamaly, I. Lavdas, E. Stevens, Q. –D. Nguyen, M. Wylezinska-Arridge, E. O. Aboagye, N. J. Long, *Angew. Chem. Int. Ed.*, 2014, **53**, 9550.
5. B. Matt, K. M. Pondman, S. J. Asshoff, B. t. Haken, B. fleury, N. Katsonis, *Angew. Chem. Int. Ed.*, 2014, **53**, 12446.
6. M. Cano, G. d. l. Cueva-Méndez, *Chem. Commun.*, 2015, DOI:10.1039/c4cc09311a.
7. G. Giakisikli, A. N. Anthemidis, *Anal. Chim. Acta*, 2013, **789**, 1.
8. S. Palacin, P. C. Hidber, J. –P. Bourgoin, C. Miramond, C. Fermon, G. M. Whitesides, *Chem. Mater.*, 1996, **8**, 1316
9. D. –M. Drotlef, P. Blűmler, A. d. Campo, *Adv. Mater.*, 2014, **26**, 775
10. P. Tseng, J. Lin, K. Owsley, J. Kong, A. Kunze, C. Murray, D. D. Carlo, *Adv. Mater.*, 2014, DOI: 10.1002/adma.201404849.
11. M. Mannini, D. Bonacchi, L. Zobbi, F. M. Piras, E. A. Speets, A. Caneschi, A. Cornia, A. Magnani, B. J. Ravoo, D. N. Reinhoudt, R. Sessoli, D. Gatteschi, *Nano Lett.*, 2005, **5**, 1435.
12. Y. Jie, J. R. Niskala, A. C. Johnston-Peck, P. J. Krommenhoek, J. B. Tracy, Huiqing. Fan, W. You, *J. Mater. Chem.*, 2012, **22**, 1962.
13. M. Cavallini, E. Bystrenova, M. Timko, M. Koneracka, V. Zavisova, P. Kopcansky, *J. Phys.: Condens. Matter*, 2008, **20**, 204144.
14. F. Hua, T. Cui, Y. Lvov, *Langmuir*, 2002, **18**, 6712.
15. G. Leem, A. C. Jamison, S. Zhang, D. Litvinov, T. R. Lee, *Chem. Commun.*, 2008, 4989.
16. M. R. Hammond, H. Dietsch, O. Pravaz, P. Schurtenberger, *Macromolecules*, 2010, **43**, 8340.

17. T. Nakanishi, Y. Masuda, K. Koumoto, *Chem. Mater.*, 2004, **16**, 3484.
18. L. An, W. Li, B. Xie, Z. Li, J. Zhang, B. Yang, *J. Colloid Interface Sci.*, 2005, **288**, 503.
19. G. Wegner, *Z. Natueforsch.*, 1969, **24**, 824.
20. X. Sun, T. Chen, S. Huang, L. Lia, H. Peng, *Chem. Soc. Rev.*, 2010, **39**, 4244.
21. O. Yarimaga, J. Jaworski, B. Yoon, J. –M. Kim, *Chem. Commun.*, 2012, **48**, 2469.
22. X. Chen, G. Zhou, X. Peng, J. Yoon, *Chem. Soc. Rev.*, 2012, **41**, 4610.
23. H. Jiang, Y. Wang, Q. Ye, G. Zou, W. Su, Q. Zhang, *Sens. Actuators: B.,* 2010, **143**, 789.
24. T. Eaidkong, R. Mungkarndee, C. Phollookin, G. Tumcharern, M. sukwattanasinitt, S. Wacharasindhu, *J. Mater. Chem.*, 2012, **22**, 5970.
25. X. Wang, X. Sun, P. A. Hu, J. Zhang, L. Wang, W. Feng, S. Lei, B. Yang, W. Cao, *Adv. Funct. Mater.,* 2013, **23**, 6044.
26. B. W. Davis, A. J. Burris, N. Niamnont, C. D. Hare, C. –Y. Chen, M. Sukwattanasinitt, Q. Cheng, *Langmuir,* 2014, **30**, 9616.
27. Q. Cheng, R. C. Stevens, *Langmuir*, 1998, **14**, 1974.
28. H. Jeon, J. Lee, M. H. Kim, J. Yoon, *Macromol. Rapid. Commuun.,* 2012, **33**, 972.
29. J. Lee, E. J. Jeong, J. Kim, *Chem. Commun.*, 2011, **47**, 358.
30. J. Lee, S. Seo, J. Kim, *Adv. Funct. Mater.*, 2012, **22**, 1632.
31. G. Yang, W. Hu, H. Xia, G. Zou, Q. Zhang, *J. Mater. Chem. A.,* 2014, **2**, 15560.
32. Y. Li, L. Wang, X. Yin, B. Ding, G. Sun, T. Ke, J. Chen, J. Yu, *J. Mater. Chem. A.,* 2014, **2**, 18304.
33. R. Pimsen, A. Khumsri, S. Wacharasindhu, G. Tumcharern, M. Sukwattanasinitt, *Biosens. Bioelectron.,* 2014, **62**, 8.
34. S. Lu, F. Luo, X. Duan, C. Jia, Y. Han, H. Huang, *J. Appl. Polym. Sci.* 2014, DOI: 10.1002/APP.40634.
35. Y. Xu, J. Le, W. Hu, G. Zou, Q. Zhang, *J. Colloid Interface Sci.,* 2013, **400**, 116.
36. S. Lee, J. Lee, M. Lee, Y. K. Cho, J. Baek, J. Kim, S. Park, M. H. Kim, R. Chang, J. Yoon, *Adv. Funct. Mater.,* 2014, **24**, 3699.
37. R. A. Nallicheri, M. F. Rubner, *Macromolecules*, 1991, **24**, 517.
38. P. Samyn, J. Rühe, M. Biesalski, *Langmuir*, 2010, **26**, 8573.
39. J. Lee, B. Yoon, D. –Y. Ham, O. Yarimaga, C. W. Lee, J. Jaworski, J. –M. Kim, *Macromol. Chem. Phys.*, 2012, **213**, 893.
40. J. Lee, H. T. Chang, H. An, S. Ahn, J. Shim, J. –M. Kim, *Nat. Commun.*, 2013, **4**, 2461.
41. J. Lee, M. Pyo, S. –h. Lee, J. Kim, M. Ra, W. –Y. Kim, B. J. Park, C. W. Lee, J. –M. Kim, *Nat. Commun.*, 2014, **5**, 3736.
42. D. H. Kang, H. –S. Jung, N. Ahn, S. M. Yang, S. Seo, K. –Y. Suh, P. –S. Chang, N. L. Jeon, J. Kim, *ACS. Appl. Mater. Interfaces*, 2014, **6**, 10631.
43. X. Liu, M. D. Kaminski, Y. Guan, H. Chen, H. Liu, A. J. Rosengart, *J. Magn. Magn. Mater.*, 2006, **306**, 248.
44. T. P. Vinod, J. H. Chang, J. Kim, S. W. Rhee, *Bull. Korean Chem. Soc.*, 2008, **29**, 799

